

Discussion

The theoretical model of an ionizing shock employed in this Note is fairly simple and can be used for calculating the shock adiabatics in monatomic gases and the maximal degree of gas compression behind the shock. Although the model takes into account only one mechanism of energy losses related to the ionization of neutral atoms, it results in good agreement with the experiment as follows from the comparison shown in Fig. 2. This means that the incorporation in the model of other energy loss mechanisms, such as the loss of energy by excitation of electron levels and by radiation cooling would be hardly expedient for calculating the ionizing shock adiabatic, at least, its increasing section. On the other hand, it should be noted that the tail part of the descending section of the shock adiabatic, for which kT_2 is of the order or larger than the difference $I_2 - I_1$, where I_2 is the second ionization potential, cannot be described satisfactorily by the present model. The reason is that in this region of equilibrium temperatures and corresponding shock Mach numbers, the ionization of single and multicharged ions should occur.

Although the fact that the compression degree by ionizing shocks in monatomic gases may considerably exceed the classic limiting value for gasdynamic shocks $\eta_m = 4$ was known in the literature (e.g., Refs. 1, 7, 8), the conditions providing for the maximal compression degree by such shocks and, furthermore, the similarity relation for η_m , were not clarified in earlier works. The reason for the occurrence of a maximum for the dependence $\eta(P)$ [or $\eta(M_1)$] is that the endothermic reaction of ionization leads to a drop of temperature and to a growth of density in the relaxation zone, so that the value of the compression degree passes through the classic limit $\eta = 4$ when M_1 increases. The descending section of the ionizing shock adiabatic appears due to the fact that there is a range of sufficiently large Mach numbers M_1 for which the plasma behind the relaxation zone becomes practically fully ionized with respect to the first ionization, while the degree of second ionization still remains small (in the calculating model the latter is neglected). As a result, a subsequent increase of M_1 leads to more rapid growth of the equilibrium temperature T_2 than in the range of lower values of M_1 , so that the equilibrium gas density ρ_2 starts to decrease. Analogous mechanisms for the formation of nonmonotonic shock adiabatics is displayed in dissociating shocks propagating in molecular gases. Examples of such adiabatics may be found in Refs. 2 and 9.

The experimental data for argon presented in Fig. 2 correspond to the increasing section of the calculated dependence $\eta(M_1)$. Griffiths et al.⁹ went beyond that limit, and indeed their experimental results indicate a maximum compression ratio $\eta_m \approx 14$ for argon at 1 Torr, occurring at a pressure ratio $P_m \approx 1500$. These results correspond to those obtained by Eqs. (1–3).

Acknowledgment

This work was sponsored by the Israel Ministry of Science, Jerusalem, Israel, under Contract 85412101.

References

- ¹Lieberman, M. A., and Velikovich, A. L., *Physics of Shock Waves in Gases and Plasmas*, Springer-Verlag, Berlin, 1986.
- ²Anderson, J. D., *Hypersonic and High Temperature Gas Dynamics*, McGraw-Hill, New York, 1989.
- ³Tsikulin, M. A., and Popov, E. G., *Radiative Properties of Shock Waves in Gases*, Moscow, Nauka, 1977 (in Russian).
- ⁴Asinovsky, E. I., Lebedev, E. F., and Ostashev, V. E., "Investigation of Processes Determining the Efficiency of Energy Conversion in a Linear Explosive MHD Generator," *Proceedings of the 7th International Conference on MHD Electrical Power Generation* (Cambridge, MA), Vol. 2, 1980, pp. 605–612.
- ⁵Lukyanov, G. A., *Supersonic Plasma Jets*, Mashinostroenie, Leningrad, 1985 (in Russian).
- ⁶Pinegre, M., These, Universite de Rouen, Mont-Saint-Aignan, France, 1976.

France, 1976.

⁷Glass, I. I., and Liu, W. S., "Effects of Hydrogen Impurities on Shock Structure and Stability in Ionizing Monatomic Gases. Part 1. Argon," *Journal of Fluid Mechanics*, Vol. 84, 1978, pp. 55–77.

⁸Kaniel, A., Igra, O., Ben-Dor, G., and Mond, M., "Ionization Behind Strong Shocks in Argon," *Physics of Fluids*, Vol. 29, No. 11, 1986, pp. 3618–3625.

⁹Griffiths, R. W., Sandeman, R. J., and Hornung, H. G., "The Stability of Shock Waves in Ionizing and Dissociating Gases," *Journal of Physics D: Applied Physics*, Vol. 9, 1976, pp. 1681–1691.

Solid Rocket Motor Temperature Sensitivity

J. R. Osborn* and S. D. Heister†
Purdue University, West Lafayette, Indiana 47907

Introduction

TEMPERATURE sensitivity refers to the influence of the initial propellant temperature on the propellant burning rate and encompasses the effect of initial temperature on the thrust and burning time of the solid propellant rocket motor. The temperature sensitivity of the propellant and the solid rocket motor are described by several different temperature sensitivity coefficients.¹ The coefficients are, the temperature sensitivity of the burning rate at constant combustion chamber pressure (a propellant composition parameter only)

$$\sigma_p = \left(\frac{\partial \ln r}{\partial T} \right)_p \quad (1)$$

the temperature sensitivity of burning rate at constant motor geometry, a constant value of the propellant area ratio² K (both a rocket motor parameter and a propellant composition parameter)

$$\sigma_K = \left(\frac{\partial \ln r}{\partial T} \right)_K \quad (2)$$

and the temperature sensitivity of the combustion chamber pressure for constant motor geometry (both a propellant composition parameter and a rocket motor parameter):

$$\pi_K = \left(\frac{\partial \ln p}{\partial T} \right)_K \quad (3)$$

Another coefficient, the temperature sensitivity of the characteristic velocity for constant motor geometry (both a propellant composition parameter and a rocket motor parameter)

$$\pi_c = \left(\frac{\partial \ln c^*}{\partial T} \right)_K \quad (4)$$

is necessary for deriving a working relationship for Eq. (3) since the characteristic velocity is involved in the equilibrium combustion chamber pressure equation.²

Received Dec. 27, 1993; revision received March 7, 1994; accepted for publication March 8, 1994. Copyright © 1994 by the American Institute of Aeronautics and Astronautics, Inc. All rights reserved.

*Professor Emeritus, School of Aeronautics and Astronautics. Associate Fellow AIAA.

†Associate Professor, School of Aeronautics and Astronautics. Member AIAA.

The coefficient of greatest interest is the motor temperature sensitivity coefficient defined by Eq. (3). Its value determines the pressure, thrust, and burning time of the motor at the temperature extremes.

Analysis

Three different relationships³⁻⁶ for the motor temperature sensitivity coefficient π_K have been derived. Derivation of π_K involves combining St. Roberts' burning rate law for defining the burning rate

$$r = cp^n \quad (5)$$

with the equilibrium combustion chamber pressure equation.² The three different equations for the motor temperature sensitivity coefficient are

$$\pi_K = [\sigma_p / (1 - n)] \quad (6)$$

from Refs. 3 and 4 and

$$\pi_K = [(\sigma_p + \pi_c) / (1 - n)] \quad (7)$$

from Ref. 5. Both Eqs. (6) and (7) assume in their derivation that

$$\sigma_K = \left(\frac{\partial \ln r}{\partial T} \right)_K = \left(\frac{\partial \ln c}{\partial T} \right)_K + \ln p \left(\frac{\partial n}{\partial T} \right)_K + n\pi_K = \sigma_p + n\pi_K \quad (8)$$

where

$$\sigma_p = \left(\frac{\partial \ln r}{\partial T} \right)_p = \left(\frac{\partial \ln c}{\partial T} \right)_p + \ln p \left(\frac{\partial n}{\partial T} \right)_p \quad (9)$$

In Eq. (8), we wrote $\sigma_K = \sigma_p + n\pi_K$ only when c and n are not functions of pressure. The third equation is

$$\pi_K = \frac{1}{1 - n} \left[\left(\frac{\partial \ln c}{\partial T} \right)_K + \ln p \left(\frac{\partial n}{\partial T} \right)_K + \pi_c \right] \quad (10)$$

from Ref. 6. No assumptions regarding the equality of $[\]_K$ and $[\]_p$ derivatives are made.

In order to utilize experimental data, the above three expressions may be written in finite difference form. Thus, from Eq. (9), Eq. (6) becomes

$$\pi_K = \frac{1}{1 - n_2} \left[\frac{\ln c_2 / c_1}{T_2 - T_1} + \ln p_1 \left(\frac{n_2 - n_1}{T_2 - T_1} \right) \right] \quad (11)$$

From Eq. (9), Eq. (7) becomes

$$\pi_K = \frac{1}{1 - n_2} \left[\frac{\ln c_2 / c_1}{T_2 - T_1} + \ln p_1 \left(\frac{n_2 - n_1}{T_2 - T_1} \right) + \pi_c \right] \quad (12)$$

The finite difference form of Eq. (10) is

$$\pi_K = \frac{1}{1 - n_3} \left[\frac{\ln c_3 / c_1}{T_2 - T_1} + \ln p_1 \left(\frac{n_3 - n_1}{T_2 - T_1} \right) + \pi_c \right] \quad (13)$$

Since most rate-pressure curves⁷ show that the pressure exponent n changes with pressure, it is of interest to compare the values of π_K as determined by the three different π_K expressions above [Eqs. (11-13)] for propellants having pressure exponent changes with pressure.

It should be noted that, at least for ammonium perchlorate-based composite propellants, the available theories, GDF,⁸ BDP,⁹ and PEM,¹⁰ predict an exponent change with pressure. Moreover, theory predicts that the burning rate curves are continuous functions of pressure, whereas the experimentally observed exponent break may possibly be an artifact of limited experimental data at a temperature. Thus, propellant burning rate curves with exponent breaks will be shown, but it should be recognized that the burning rate curve may be considered continuous with gradual exponent changes, and that the burning rate exponent n is the slope of the curve at a point or pressure. From that slope at that point, the corresponding value of the parameter c may be determined, thereby enabling Eq. (5) to be used at any point.

Numerical Examples

Two different propellants, as illustrated in Figs. 1 and 2, will be utilized in comparing the values of π_K as determined using Eqs. (11-13). The values for the rate parameters of the two propellants are shown in Table 1. The value of π_c will be assumed constant.¹¹ Thus, $\pi_c = 0.00006$. The values for the two temperatures are 1) $T_1 = 70^\circ\text{F}$ and 2) $T_2 = 145^\circ\text{F}$, and the value of p_1 is 1400 psia, the motor operating pressure at the lower temperature.¹¹

For both propellants an exponent break occurs for the higher temperature at 1500 psia. Consequently, the parameter n for that branch is a function of pressure, as is the parameter c . In the first case the value of the exponent increases after the

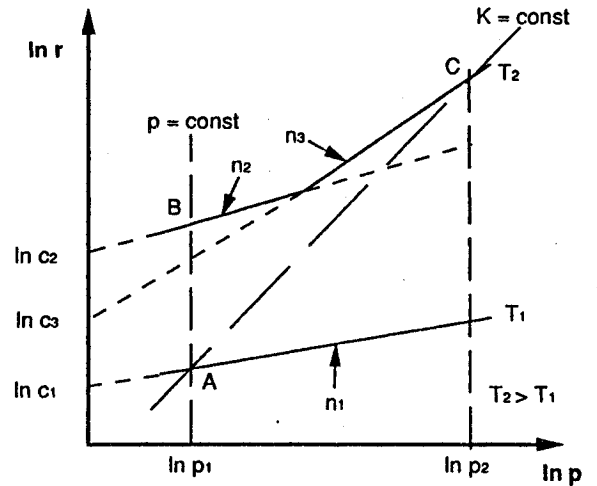


Fig. 1 Schematic of burning rate behavior of propellant 1.

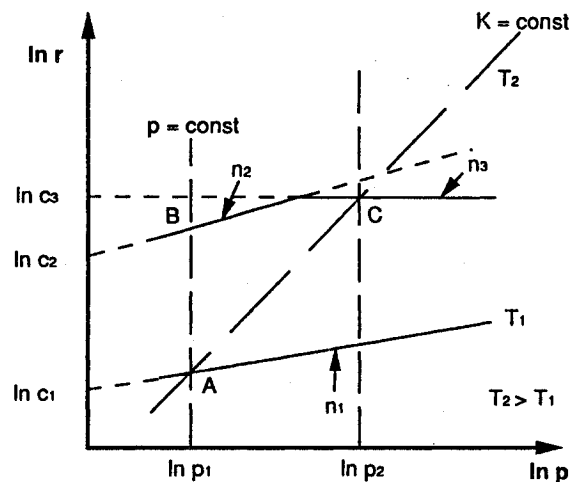


Fig. 2 Schematic of burning rate behavior of propellant 2.

Table 1 Burning rate parameters

	Propellant 1 ¹¹		Propellant 2	
	<i>c</i>	<i>n</i>	<i>c</i>	<i>n</i>
Burning rate branch, subscript 1	0.050357	0.3	0.050357	0.3
Burning rate branch, subscript 2	0.026880	0.4	0.026880	0.4
Burning rate branch, subscript 3	0.0029964	0.7	0.5010	0.0

Table 2 π_K values

	Eq. (11)	Eq. (12)	Eq. (13)
Propellant 1	0.002149	0.002248	0.003576
Propellant 2	0.002149	0.002248	0.001716

Table 3 P_2 values, psia

	Equation	Eq. (14)	True value
Propellant 1 Figure 1	(11)	1644	1830
	(12)	1657	
	(13)	1830	
Propellant 2 Figure 2	(11)	1644	1593
	(12)	1657	
	(13)	1593	

break, whereas in the second case it decreases. Conversely, the parameter *c* decreases for the first and increases for the second.

On each figure the line A-B represents a line of constant pressure, and the line A-C represents a line in which *K* is constant. At the low temperature T_1 the rocket motor operates at point A, while point C represents the motor operating point at the high temperature T_2 .

Substituting the proper values for the rate parameters into Eqs. (11–13) from the values for the two propellants yields the values shown in Table 2.

From the definition of π_K , Eq. (3), the equilibrium combustion chamber pressure in the rocket motor at the elevated temperature may be written

$$p_2 = p_1 \exp[(T_2 - T_1)\pi_K] \quad (14)$$

Substituting the values from the results of the calculations of π_K yields the values shown in Table 3. The true value of p_2 in the third column of Table 3 is calculated from the equilibrium combustion chamber equation² using the proper values for c^* , *c*, and *n* at T_2 .

As can be seen, the values predicted for both π_K and the final equilibrium combustion chamber pressure p_2 , differ for the three different relationships, Eqs. (6), (7) and (10). Also, the values predicted by Eqs. (6) and (7) are identical for the two propellants regardless of the value of the exponent after the exponent break. The values predicted by Eq. (10) differ for the two propellants as they should.

Discussion

The three expressions for π_K have been shown to yield different numerical results for the most general case in which the propellant has exponent breaks. Similar differences would be found for a propellant with gradual changes in exponent with pressure. The reason for the difference is that the motor temperature sensitivity coefficients [Eqs. (6) and (7)] assume that the burning rate parameters *c* and *n*, are not functions of pressure [see Eqs. (8) and (9)]. As a result of this assumption, the π_K expression of Eqs. (6) and (7) involves the parameter σ_p , which is by definition restricted to burning rate

changes with temperature in which the pressure remains constant. As a result, neither Eq. (6) nor Eq. (7) can predict the effects that occur at higher pressures. In fact, Eqs. (6) and (7), predict values of π_K and p_2 that are identical for both propellants regardless of the value of the burning rate exponent at the higher temperature.

The temperature sensitivity coefficient described by Eq. (10) has been derived for the case in which both burning rate parameters *c* and *n*, are assumed to be functions of temperature and pressure. Equation (10) involves the partial derivatives with the motor geometry held constant. Therefore, it represents the motor operation at the different temperatures for the most general case in which the exponent changes with pressure, and its value depends upon the final value of the exponent at the higher temperature.

Conclusions

The three expressions for π_K were shown to be of equal complexity and ease of use. All involve only the data taken for burning rate and use the parameters in St. Roberts' burning rate law. The most general expression for the motor temperature sensitivity coefficient [Eq. (10)] should be used since it is a true π_K relationship having the partial derivatives taken with the motor geometry held constant.

References

- ¹Geckler, R. D., and Sprenger, D. F., "The Correlation of Interior Ballistics Data for Solid Propellants," *Jet Propulsion*, Vol. 24, No. 1, 1954, pp. 22–26.
- ²Barrere, M., Taumotte, A., Friaris de Veubeke, B., and Vandekerckhove, J., *Rocket Propulsion*, Elsevier, New York, 1960, pp. 237–242.
- ³Sutton, G. P., *Rocket Propulsion Elements*, 6th ed., Wiley, New York, 1992, pp. 377, 378.
- ⁴Kubota, N., *Fundamentals of Solid Rocket Propellant Combustion*, edited by K. K. Kuo and M. Summerfield, Vol. 90, Progress in Aeronautics and Astronautics, AIAA, New York, 1984, pp. 515–598, Chap. 10.
- ⁵Brooks, W. T., and Miller, R. R., "Relationships Among Solid Propellant Temperature Sensitivity Parameters," *Proceedings of the 1981 JANNAF Combustion Meeting*, Vol. III, 1981, pp. 277–284 (CPA 347).
- ⁶Hamke, R. E., and Osborn, J. R., "Relationships for Motor Temperature Sensitivity," *Journal of Propulsion and Power*, Vol. 8, No. 3, 1992, pp. 723–725; also Hamke, R. E., and Osborn, J. R., "Relationships for Motor Temperature Sensitivity" (Errata), *Journal of Propulsion and Power*, Vol. 10, No. 1, 1994, p. 136.
- ⁷Foster, R. L., Condon, J. A., and Dale, R. J., "Low Exponent Technology," Hercules, Allegany Ballistics Lab., Air Force Rocket Propulsion Lab., Final Rept. AFRPL-TR-82-060, Cumberland, MD, Dec. 1982.
- ⁸Summerfield, M., et al., "Burning Mechanism of Ammonium Perchlorate Propellants," *ARS Progress in Astronautics and Rocketry*, Vol. 1: *Solid Propellant Rocket Research*, Academic Press, New York, 1960, pp. 141–182.
- ⁹Beckstead, M. W., Derr, R. L., and Price, C. F., "A Model of Composite Solid Propellant Combustion Based on Multiple Flames," *AIAA Journal*, Vol. 8, No. 12, 1970, pp. 2200–2207.
- ¹⁰Renie, J. P., Condon, J. A., and Osborn, J. R., "Oxidizer Distribution Effects on Propellant Combustion," *AIAA Journal*, Vol. 17, No. 8, 1979, pp. 877–883.
- ¹¹Glick, R. L., and Brooks, W. T., personal communication, June 1992.